Journal of Southeast University (English Edition) Vol. 22, No. 1, pp. 125 – 129 Mar. 2006 ISSN 1003—7985

Oxide/substrate interfacial defects in high temperature oxidation of Co-40Cr by acoustic emission method

Jin Huiming[1] Zhang Jianfeng[1] Adriana C. Felix[2] Majorri H. Aroyave[2]

([1]College of Mechanical Engineering, Yangzhou University, Yangzhou 225009, China)

([2] College of Materials Engineering, National University of Antiuquia, Medellin 23715, Colombia)

Abstract: The isothermal oxidation kinetics of a Co-40Cr alloy and its yttrium ion-implanted samples were studied at 1 000 ℃ in air by thermal-gravity analysis (TGA). Scanning electronic microscopy (SEM) was used to examine the Cr_2O_3 oxide film's morphology after oxidation. An acoustic emission (AE) method was used in situ to monitor the cracking and spalling of oxide films formed on samples during oxidation and subsequent air-cooling stages. A theoretical model was proposed relating to the film fracture process and was used to analyze the acoustic emission spectrum on time domain and the AE-event number domain. It was found that yttrium implantation remarkably reduced the isothermal oxidation rate of Co-40Cr and improved the anti-cracking and anti-spalling properties of Cr_2O_3 oxide film. The reasons for the improvement were mainly that the implanted yttrium reduced the grain size of Cr_2O_3 oxide, increased the high temperature plasticity of oxide film, and remarkably reduced the number and size of Cr_2O_3/Co-40Cr interfacial defects.

Key words: oxidation; acoustic emission; element binding energy; interface; yttrium

The resistance of high temperature alloys to an oxidation environment depends on the formation of slowly growing and adherent oxide films. Usually there are intrinsic growing stress and external thermal stress formed in oxide films[1,2]. The former may arise from the volume changes when the metal is oxidized to oxide, while the latter may arise from the thermal expansion difference between the metal and the oxides. Many studies[1-8] have been carried out relating to the isothermal and cyclic oxidation behaviors of different super-alloys and high temperature coatings, and several methods have been developed to measure the residual stresses inside the oxide films, because the residual stress level may be a critical factor influencing the cracking and spalling of oxide films. Cobalt based super-alloy is widely used in high temperature environments due to its excellent mechanical and anti-oxidation properties. In this paper, an acoustic emission method is used to monitor the cracking and spalling of oxide film formed on Co-40Cr alloy during high temperature oxidation. A related mechanical and mathematical model is proposed to study the Cr_2O_3/Co-40Cr interfacial defects' distribution, and finally the influence of yttrium ion-implantation on the high temperature oxidation of Co-40Cr is evaluated by this method and other oxide structure analysis methods.

Received 2005-04-13.

Biography: Jin Huiming (1968—), male, doctor, professor, doctorjhm@sohu.com.

1 Experiment

The Co-40Cr alloy was wire-cut into 10 mm × 10 mm × 1 mm samples which were ultimately polished by 0.2 μm Al_2O_3 abrasive paste. After being ultrasonically cleaned in acetone and alcohol, some specimens were ion-implanted 3×10^{17} Y^+/cm^2 yttrium using an MEVVE-8010 ion-implantation machine. The isothermal oxidation experiment was carried out at 1 000 ℃ in air in an M25DV thermal balance to study the oxidation kinetics of the Co-40Cr and the Y-implanted Co-40Cr alloy. In the acoustic emission experiment, Y-free and Y-containing specimens were point-welded to platinum wave-guides (2 mm in diameter) respectively which were connected to an AE-100 acoustic emission apparatus, the schematic diagram of the experiment is shown in Fig. 1.

These specimens were isothermally oxidized at

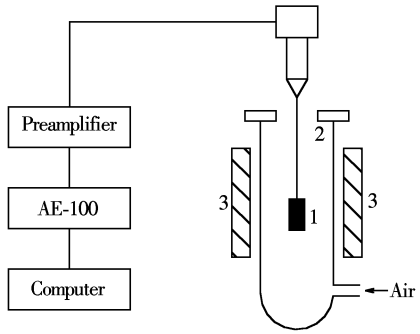

1— Sample; 2— Pt wave guide; 3— Furnace

Fig. 1 Schematic diagram of the acoustic emission experiment

1 000 ℃ in air for 90 h and then air-cooled to room temperature. During the whole process acoustic emission (AE) signals were monitored in situ using the AE-100 unit with a threshold voltage of 84 dB. Scanning electronic microscopy (SEM) was used to examine the surface morphology of oxide films.

2 Results and Discussion

The isothermal oxidation mass-gain curves of the Co-40Cr and Y-implanted Co-40Cr are shown in Fig. 2. It can be seen that yttrium implantation greatly reduced the oxidation rate of the Co-40Cr alloy.

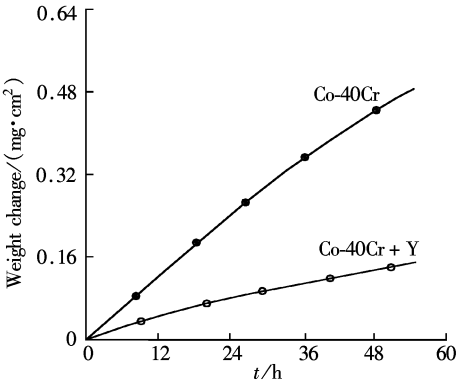

Fig. 2 Isothermal oxidation mass-gain curves of Co-40Cr and Y-implanted Co-40Cr

Fig. 3 shows the SEM morphologies of the oxide films formed on Co-40Cr and its Y-implanted samples after 24 h isothermal oxidation. We can find that yttrium ion-implantation remarkably reduced the grain size of oxide film, and ridge character had apparently arisen in the Y-containing oxide film (see Fig. 3(b)). Energy dispersive spectrum (EDS) analysis showed that the oxide films formed on two kinds of samples were both pure Cr_2O_3, and this was due to the high Cr content and its preferential oxidation in Co-Cr binary alloy. The mechanism of the rare earth effects (REE) on Cr_2O_3 (and even NiO) oxide-forming alloys during high temperature oxidation was studied in other papers[3,4] and would be explained later. In these works secondary ion mass spectrum (SIMS) and high resolution electronic microscopy (HREM) were used to study the chromium bonding energy change and the yttrium segregation.

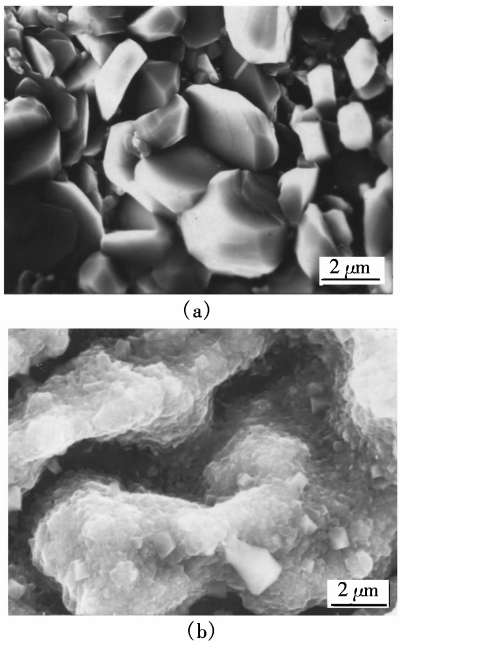

Fig. 3 SEM morphologies of oxide films formed after 24 h isothermal oxidation. (a) Co-40Cr; (b) Y-implanted Co-40Cr

In the acoustic emission experiment, almost no AE signal was detected during the 90 h isothermal oxidation stage, while in the air-cooling stage many AE signals were detected as shown in Fig. 4.

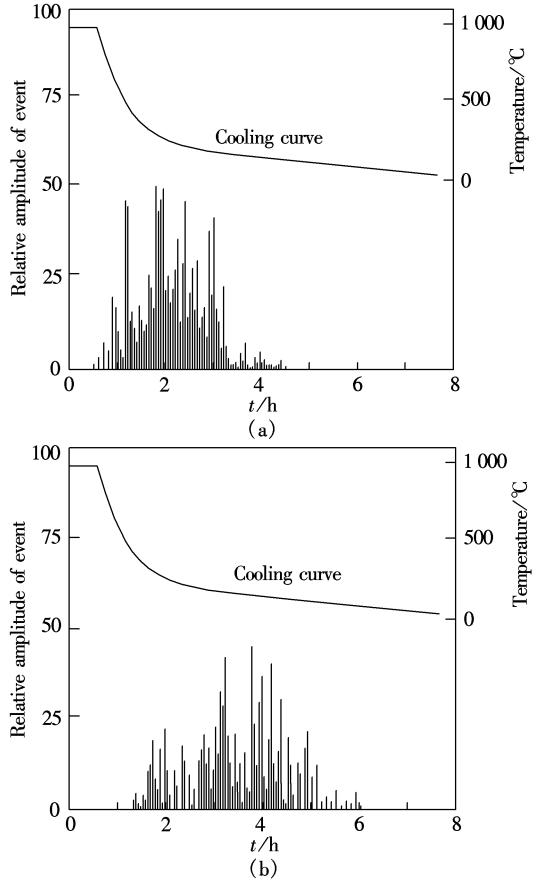

Fig. 4 AE signal distributions measured in air-cooling stage after 90 h isothermal oxidation. (a) Co-40Cr; (b) Y-implanted Co-40Cr

During the isothermal oxidation stage, the growth stress σ_{gw} is caused by volume change when the metal was oxidized to its oxide, which can be quantitatively correlated to a Pilling-Bedworth ratio (PBR) (volume of oxide/volume of metal consumed). For chromium, this value is 1.57 and the internal growth stress within the Cr_2O_3 oxide film is compressive[2]. During the air-cooling stage, thermal stress is generated due to the

linear thermal expansion difference between Cr_2O_3 and substrate metal. This thermal stress σ_{th} is also compressive and can be expressed as

$$\sigma_{th} = \frac{E_{OX}\Delta T(\alpha_M - \alpha_{OX})}{1-\nu} \quad (1)$$

where E_{OX} is the Young's modulus of the oxide; ν is the Poisson's ratio of the oxide; α_M and α_{OX} are the thermal expansion coefficients of the metal and oxide, respectively; ΔT is the temperature change. So the total compressive stress σ_{OX} in the oxide film can be expressed as

$$\sigma_{OX} = \sigma_{gw} + \frac{E_{OX}\Delta T(\alpha_M - \alpha_{OX})}{1-\nu} \quad (2)$$

In most cases, the first term in the right side of Eq. (2) is much smaller than the second term, and can be omitted[2].

The number of AE signals detected in the oxidation stage and air-cooling stage can be expressed as a function of temperature change, $n = f(\Delta T)$, where n is the number of AE signals collected in a given time interval. According to Zhang's simplification[5], the spalling of oxide above one interfacial defect can generate Z AE events, of which $Z-1$ from through-thickness cracking along the perimeter of the buckled oxide and 1 from the final spalling, and usually Z is an integer between 5 and 8. Then the number of interfacial defects in a given ΔT interval can be expressed as

$$N = \frac{n}{Z} = \frac{f(\Delta T)}{Z} \quad (3)$$

According to Ref. [1], the oxide film spalling process should be preceded by a film buckling process above an interfacial defect. When the accumulative compressive stress inside the oxide film reaches a critical value, oxide film buckling will occur above interfacial defects. The compressive stress in the buckled region is partially relieved, while the concentrated stress at the perimeter of this region will cause propagation of crack tip towards the outer face of oxide film, and will finally result in through-thickness cracking and spalling of oxide film. The interfacial defect formation processes and oxide film spalling processes are schematically shown in Fig. 5. The quantitative description for the critical stress condition can be expressed as

$$\sigma_{OX} = \frac{3.6H^2E_{OX}^2}{C^2} \quad (4)$$

where H is the thickness of the oxide film and C is the radii of the interfacial defect (i. e. the radius of the local spalled region). This equation implies that each interfacial defect with different radii will spall under different compressive stress levels. So local oxide upon a large interfacial defect will crack and spall at a small ΔT drop, while oxide upon small interfacial defects will crack and spall at larger ΔT drops, this is also experimentally confirmed from the AE signal spectrum in Fig. 4.

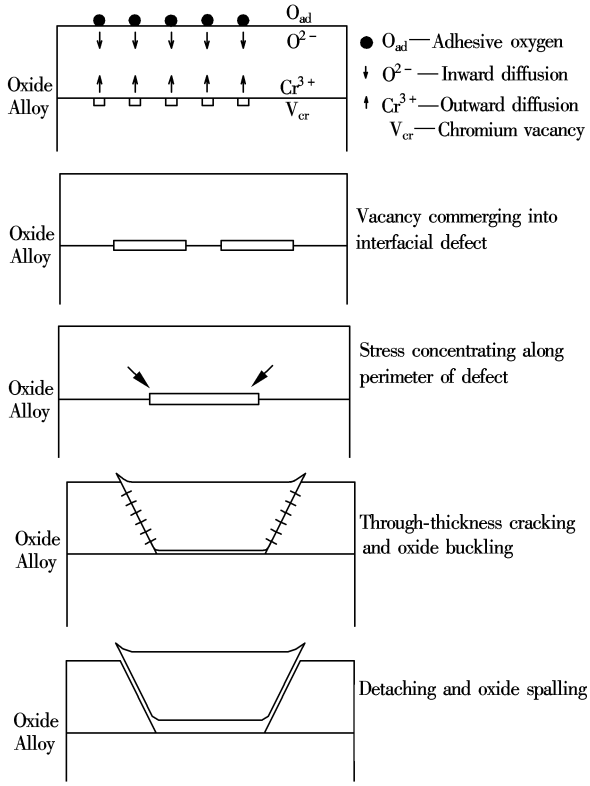

Fig. 5 Schematic diagram of interfacial defect formation and cracking and spalling of oxide film upon interfacial defect

By combining Eqs. (2), (3) and (4) and omitting σ_{gw}, we get

$$C = 1.9H\left(\frac{E_{OX}(1-\nu)}{\Delta T(\alpha_M - \alpha_{OX})}\right)^{\frac{1}{2}} \quad (5)$$

$$N = \frac{1}{Z}f\left(3.6\,\frac{E_{OX}H^2(1-\nu)}{C^2(\alpha_M - \alpha_{OX})}\right) \quad (6)$$

The Young's modulus E_{OX} and the Poisson's ratio ν for Cr_2O_3 oxide are 153 GPa and 0.32, respectively; linear thermal expansion coefficient α_M and α_{OX} for Co-40Cr and Cr_2O_3 are 0.14 K^{-1} and 0.026 K^{-1}, respectively[6,7] (all the above data are averagely taken at 750 ℃). The thickness of Cr_2O_3 oxide films can be calculated from the mass-gain curves shown in Fig. 2, and Z is set to integer 6 in our oxide fracture model.

By converting the measured distribution of AE signals in time domain to temperature domain using Hi-Draw 2.1 software in AE-100 acoustic emission apparatus and by differential calculation of the number of AE signals on temperature domain using Eqs. (5) and (6), we can finally get the interfacial defect number distribution (N) vs. defect size (i. e. radius C) as shown in Fig. 6.

From Fig. 6 we can find that the interfacial

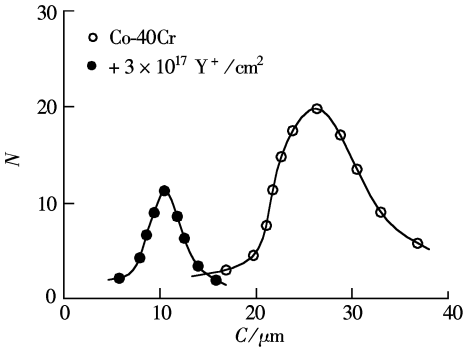

Fig. 6 Number distribution of interfacial defects vs. defect size

defects' number distribution vs. defect size follows roughly the law of Gaussian distribution, and the average interfacial defect radii for Co-40Cr and Y-implanted Co-40Cr are 27.0 μm and 10.5 μm, respectively. Meanwhile, Y-implantation reduced the total number of interfacial defects, which can be seen by a comparing the areas under the two distributional curves in Fig. 6.

SEM morphologies of Cr_2O_3 oxide films formed on Co-40Cr and Y-implanted Co-40Cr after 90 h isothermal oxidation are shown in Fig. 7. We can see that severe spallation occurred in oxide film formed on Co-40Cr in Fig. 7(a), while few spalled regions are found in oxide films formed on Y-implanted Co-40Cr in Fig. 7(b).

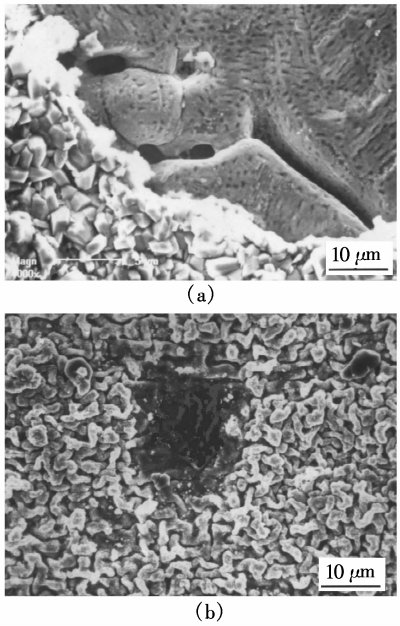

Fig. 7 SEM morphologies of oxide films formed after 90 h isothermal oxidation. (a) Co-40Cr; (b) Y-implanted Co-40Cr

The reasons for the improved property of Cr_2O_3 film in anti-cracking and anti-spallation caused by yttrium ion-implantation can be explained in two ways. First, yttrium implantation greatly reduced the internal compressive stress level in the Cr_2O_3 film. Usually the maximum depth of ion-implantation was less than 100 nm and the local concentration of yttrium was rather high, meanwhile, ion-implantation introduced large amounts of dislocations in alloy surface[3]. During the initial oxidation stage, high concentration and high chemical activity of yttrium in alloy surface promoted fine-grained Cr_2O_3 oxide crystal formation.

From Fig. 3(b) we can find apparent grain-size refining effect and ridge character in Y-doped Cr_2O_3 oxide film, this kind of fine-grained oxide film has better high temperature plasticity and creeping property, which means that Cr_2O_3 oxide film can relieve parts of internal compressive stress by means of high temperature creeping rather than by means of cracking and spalling. This oxide grain-refining effect is due to the high local concentration and high chemical activity of yttriuml; i. e. yttrium might act as the Cr_2O_3 crystal forming site during the initial oxidation stage. The actual existing form of implanted yttrium within Cr_2O_3 oxide film could be very fine Y_2O_3, $YCrO_3$ spinel particles or even Y^{3+} ions located at Cr_2O_3 grain boundaries[3,8].

Secondly, yttrium implantation remarkably reduced the number and size of interfacial defects as shown in Fig. 6 and greatly improved the Cr_2O_3/Co-40Cr interfacial adhesive property. Statistic examination of a size of about 100 spalled areas of Y-free and Y-containing Cr_2O_3 oxide films in our experiment by the SEM method indicated that the average defect size tested by the AE method was about 1.5 to 2.0 times larger than the SEM-observed average size of the spalled regions. The reason for the higher AE-tested value of interfacial defect size was probably due to the interaction between nearby existing defects, since the stress relief of one defect would have a great influence on the near-located defects' stress status. In addition, the choosing of values as the Young's modulus, the Poisson's ratio and the thermal expansion coefficient of oxide with different micro-structures at different temperatures might be another reason for the higher AE-tested average defect size.

Although it is difficult to propose very accurate mechanical models to study the cracking and spallation of oxide films, the acoustic emission technique still seems to be a promising method and is used by some researchers[5,8]. Further detailed investigation by this method is needed and must be done in association with other oxidation research methods.

3 Conclusions

1) Yttrium ion-implantation remarkably reduced the isothermal oxidation rate of Co-40Cr; meanwhile, the anti-cracking and anti-spalling properties of the Cr_2O_3 oxide film were greatly improved by Y-implantation. These rare earth effects were mainly attributed to the lower internal stress level, the grain-size refining effect and the improved high temperature plasticity and creeping property of Cr_2O_3 oxide film.

2) Y-implantation reduced the number and size of oxide/substrate interfacial defects and improved the adhesive property of oxide film. By using proper mechanical and mathematical methods to simulate the fracture process of oxide film, acoustic emission seems to be a promising method in quantitatively examining oxide/substrate interfacial behavior.

References

[1] Evans A G, Cannon R. Stress and decohesion of oxide scales [J]. *Materials Science Forum*, 1989, **43**(3): 243 – 249.

[2] Rahmel A, Schutze M. Mechanical aspects of rare earth effects [J]. *Oxidation of Metals*, 1992, **38**(2): 314 – 319.

[3] Jin Huiming, Li Tiefan, Li Meishuan, et al. Influence of yttrium implantation on oxidation behavior of Co-40Cr alloy [J]. *Journal of Rare Earths*, 1999, **17**(1): 34 – 38.

[4] Jin Huiming, Chen Rongfa, Zhang Linnan, et al. High temperature oxidation behavior of magnetically sputtered Ni-0.5Y micro-crystal coating [J]. *Journal of Southeast University*: *English Edition*, 2003, **19**(4): 364 – 367.

[5] Zhang Yifan, Shores D, Rahmel A, et al. Spallation of oxide scales formed on Ni-30Cr alloy [J]. *Oxidation of Metals*, 1993, **40**(1): 529 – 536.

[6] Jin Huiming, Zhang Linnan, Li Meishuan, et al. Rare earth effects on adhesion of Cr_2O_3 oxide scale formed on surface of Co-40Cr alloy [J]. *Journal of Rare Earths*, 2001, **19**(1): 34 – 39.

[7] Przybilla W, Schutze M. Role of growth stresses on the structure of oxide scales on nickel at 800 and 900 ℃ [J]. *Oxidation of Metals*, 2002, **58**(1): 103 – 145.

[8] Ul-Hamid A. Study of the effect of Y on the scale microstructures of Cr_2O_3- and Al_2O_3-forming alloys [J]. *Oxidation of Metals*, 2002, **58**(1): 23 – 45.

声发射方法研究 Co-40Cr 合金高温氧化过程的膜/基界面缺陷

靳惠明[1] 张剑峰[1] Adriana C. Felix[2] Majorri H. Aroyave[2]

([1] 扬州大学机械工程学院,扬州 225009)

([2] 哥伦比亚国立安第克大学材料工程学院,哥伦比亚麦德林 23715)

摘要:用热重分析(TGA)研究了 Co-40Cr 合金及其离子注钇样品在 1 000 ℃空气中的恒温氧化动力学规律. 用扫描电镜(SEM)对不同样品表面 Cr_2O_3 氧化膜的形貌进行了观测. 用声发射(AE)方法对合金表面氧化膜在恒温生长阶段和空冷阶段的开裂与剥落进行了实时监测,根据相应的氧化膜开裂模型,对声发射信号在时域和数域上的分布情况进行了分析. 结果表明离子注钇降低了 Co-40Cr 合金的恒温氧化速率,并提高了合金表面 Cr_2O_3 氧化膜的抗开裂和抗剥落性能. 离子注钇提高合金抗氧化性能的主要原因在于钇细化了合金表面 Cr_2O_3 氧化膜的晶粒,提高了氧化膜的高温塑性和蠕变能力,并且显著降低了 Cr_2O_3/Co-40Cr 界面缺陷的数量和大小.

关键词:氧化;声发射;元素结合能;界面;钇

中图分类号:TG174.453